

# High-field magnetization and magnetic phase transition in $\text{CeOs}_2\text{Al}_{10}$

Akihiro Kondo<sup>1,\*</sup>, Junfeng Wang<sup>1,2</sup>, Koichi Kindo<sup>1</sup>, Yuta Ogane<sup>3</sup>, Yukihiro Kawamura<sup>3</sup>, Sakiyo Tanimoto<sup>3</sup>, Takashi Nishioka<sup>3</sup>, Daiki Tanaka<sup>4</sup>, Hiroshi Tanida<sup>4</sup>, and Masafumi Sera<sup>4</sup>

<sup>1</sup>*Institute for Solid State Physics, University of Tokyo, Kashiwa, Chiba 277-8581, Japan*

<sup>2</sup>*Wuhan High Magnetic Field Center, Huazhong University of Science and Technology, Wuhan 430074, China*

<sup>3</sup>*Graduate school of Integrated Arts and Science, Kochi University, Kochi 780-8520, Japan and*

<sup>4</sup>*Department of Quantum Matter, AdSM, Hiroshima University, Higashi-hiroshima 739-8530, Japan*

(Dated: January 20, 2013)

We have studied the magnetization of  $\text{CeOs}_2\text{Al}_{10}$  in high magnetic fields up to 55 T for  $H \parallel a$  and constructed the magnetic phase diagram for  $H \parallel a$ . The magnetization curve shows a concave  $H$  dependence below  $T_{\text{max}} \sim 40$  K which is higher than the transition temperature  $T_0 \sim 29$  K. The magnetic susceptibility along the  $a$ -axis,  $\chi_a$  shows a smooth and continuous decrease down to  $\sim 20$  K below  $T_{\text{max}} \sim 40$  K without showing an anomaly at  $T_0$ . From these two results, a Kondo singlet is formed below  $T_{\text{max}}$  and coexists with the antiferro magnetic order below  $T_0$ . We also propose that the larger suppression of the spin degrees of freedom along the  $a$ -axis than along the  $c$ -axis below  $T_{\text{max}}$  is associated with the origin of the antiferro magnetic component.

PACS numbers: 75.30.Mb, 75.20.Hr, 71.27.+a

$\text{CeT}_2\text{Al}_{10}$  ( $T=\text{Ru, Os, Fe}$ ) have recently attracted much attention because of their unusual physical properties.<sup>1-16</sup> These compounds belong to the category of the Kondo semiconductor. The most characteristic feature in this system is that  $\text{CeRu}_2\text{Al}_{10}$  and  $\text{CeOs}_2\text{Al}_{10}$  exhibit an unusual long range order (LRO). These two compounds exhibit a large anisotropy of the magnetic susceptibility,  $\chi$ ;  $\chi_a > \chi_c > \chi_b$ . Here,  $\chi_a$  etc. indicates  $\chi$  along the  $a$ -axis, etc. From their temperature dependences, these two compounds are categorized into roughly localized system. The LRO temperature of  $T_0 \sim 30$  K is extremely high in comparison with  $T_N$  of other  $\text{RT}_2\text{Al}_{10}$  ( $R=\text{rare-earth element}$ ).  $T_N$  is equal to 16.5 K even in  $\text{GdRu}_2\text{Al}_{10}$ . Among  $\text{CeT}_2\text{Al}_{10}$  compounds,  $\text{CeRu}_2\text{Al}_{10}$  is most intensively studied. At the early stage, Tanida *et al.* proposed a singlet ground state from the following results. (1) A large magnetic entropy released at  $T_0$ , (2) A decrease in the magnetic susceptibility along all the crystal axes below  $T_0$ , (3) A positive pressure effect on  $T_0$  in addition to the activation-type  $T$  dependence of the physical properties.<sup>5</sup> We confirmed the magnetic origin from the high field magnetization measurement of  $\text{CeRu}_2\text{Al}_{10}$  and obtained the magnetic phase diagram.<sup>9</sup> Although a spin gap with an excitation energy of 8 meV, consistent with the singlet ground state, was observed by inelastic neutron scattering,<sup>10</sup> soon after, the magnetic ordering was reported.<sup>11</sup> The antiferro magnetic (AFM) order is characterized by an AFM moment ( $M_{\text{AF}}$ ) of  $\sim 0.34\mu_B/\text{Ce}$  parallel to the  $c$ -axis.<sup>11</sup> Although it is now confirmed that the magnetic ordering with  $M_{\text{AF}} \parallel c$  is realized below  $T_0$ , the magnetic ordered state is definitely not a simple one and there exist many unusual properties; a very high  $T_0$  despite a small ordered moment, no metamagnetic transition despite the existence of a large spin gap without a low energy magnetic excitation, the magnetic order with  $M_{\text{AF}} \parallel c$  even though  $\chi_a$  is much larger than  $\chi_c$  in the paramagnetic region.

$\text{CeOs}_2\text{Al}_{10}$  exhibits physical properties similar to those of  $\text{CeRu}_2\text{Al}_{10}$  and the same type of magnetic order is expected to be realized below  $T_0$ . On the other hand, there exist the following differences.<sup>3,12,13</sup>  $T_0$  is equal to 28.7 K which is a little higher than that of  $\text{CeRu}_2\text{Al}_{10}$ , the magnetic entropy released

at  $T_0$  and the magnitude of the ordered moment are smaller than those in  $\text{CeRu}_2\text{Al}_{10}$ ,  $\chi_a$  and  $\chi_c$  in the paramagnetic region exhibit a broad maximum at  $T_{\text{max}} \sim 40$  K in  $\text{CeOs}_2\text{Al}_{10}$ , the spin gap energy is 11 meV<sup>12</sup> which is higher than 8 meV in  $\text{CeRu}_2\text{Al}_{10}$ .<sup>10</sup> By applying pressure to  $\text{CeRu}_2\text{Al}_{10}$ , the physical properties are changed from a nearly localized regime to valence fluctuation regime as in  $\text{CeFe}_2\text{Al}_{10}$ .<sup>3</sup>  $\text{CeOs}_2\text{Al}_{10}$  is situated just between these two compounds limits.

To clarify the origin of the above differences between the two compounds, we measured the high field magnetization of  $\text{CeOs}_2\text{Al}_{10}$ .

The single crystals of  $\text{CeT}_2\text{Al}_{10}$  ( $T = \text{Ru, Os}$ ) used in the present study were prepared by the Al self-flux method. Pulsed magnetic fields up to 55 T were generated with a duration of 36 ms using non destructive magnets. Magnetization ( $M$ ) was measured by the induction method using a standard pick-up coil in magnetic fields along the  $a$ -axis. The pressure effect of  $M$  for  $H \parallel a$  was also measured using a piston cylinder type pressure cell.

Figures 1(a) and (b) represent the  $M$ - $H$  curves of  $\text{CeOs}_2\text{Al}_{10}$  under various temperatures and the  $T$  dependences of  $M$  under various magnetic fields for  $H \parallel a$ , respectively. The latter are obtained by using the results in Fig.1(a). At  $T=1.3\text{K}$ ,  $M$  shows an  $H$ -linear increase up to  $\sim 30$  T and above  $\sim 30$  T, a concave  $H$  dependence is observed. After showing an anomaly at  $H_c^{\text{I-II}}=47$  T,  $M$  increases steeply and shows a saturated behavior at  $H_c^{\text{P}}=52$  T.  $M$  at  $H_c^{\text{P}}$  is  $0.95\mu_B/\text{Ce}$  which is smaller than  $1.3\mu_B/\text{Ce}$  in  $\text{CeRu}_2\text{Al}_{10}$ .<sup>9</sup> Above 20 K, an anomaly at  $H_c^{\text{I-II}}$  could not be recognized in the present experiments. We note that although  $M$ - $H$  curves in the paramagnetic region above 40 K are normal, those at  $T=30$  K and 35 K show a concave  $H$  dependence even in the paramagnetic region, which is shown in Fig. 3 (a) in an expanded scale. Such an  $H$  dependence is not observed in  $\text{CeRu}_2\text{Al}_{10}$  above  $T_0$ .<sup>9</sup> As will be mentioned later, this different behavior of  $M$ - $H$  above  $T_0$  between two compounds is observed as a different  $T$  dependence of  $\chi_a$  above  $T_0$ . The  $T$  dependences of  $M$  in magnetic fields between 10 T and 45 T are plotted on Fig. 1(b) and show a broad maximum several Kelvin above  $T_0$

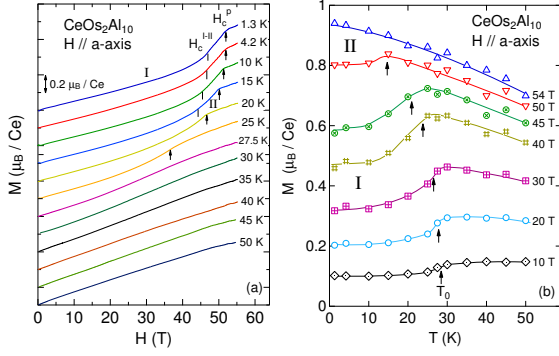


FIG. 1. (Color online) (a) Magnetic field dependence of the magnetization of  $\text{CeOs}_2\text{Al}_{10}$  under various temperatures for  $H \parallel a$ -axis. The origin of the vertical axis of each curve is shifted. The ordered state is divided into two phases I and II. (b) Temperature dependence of the magnetization under various magnetic fields for  $H \parallel a$ -axis. They are plotted by using the results in Fig. 1(a). The arrow indicates the transition temperature  $T_0$ , which is cited from the magnetic phase diagram shown in Fig. 2.

as was observed in the  $\chi$ - $T$  curve measured at low magnetic fields. No clear anomaly is seen at  $T_0$ . At  $H=50$  T, a maximum is seen at  $T_0=16$  K and the  $T$  dependence of  $M$  below  $T_N$  is weak, different from a continuous decrease observed below  $H=45$  T. The  $T$  dependence at  $H=54$  T is that observed in a usual magnetic compound in the paramagnetic region. Thus, the  $H$  region above  $H_c^p$  is considered to be paramagnetic. This is also supported by the results of  $\text{Ce}_x\text{La}_{1-x}\text{Ru}_2\text{Al}_{10}$ .<sup>5,9</sup>  $T_0$  and  $H_c^p$  is reduced roughly in proportional to La concentration toward  $x \sim 0.5$  and disappear.<sup>5</sup>

The magnetic phase diagram of  $\text{CeOs}_2\text{Al}_{10}$  for  $H \parallel a$ -axis obtained from the results in Fig. 1(a) is shown in Fig. 2. The inset shows the  $M$ - $H$  curve and  $H$  dependence of  $dM/dH$  at  $T=1.3$  K. Two anomalies are clearly seen at  $H_c^{I-II}=47$  T and  $H_c^p=52$  T. The magnetic phase diagram is similar to that of  $\text{CeRu}_2\text{Al}_{10}$ .<sup>9</sup> Hereafter, we call two LRO phases below and above  $H_c^{I-II}$  as phase I and II, respectively. The region of phase II is narrower than that in  $\text{CeRu}_2\text{Al}_{10}$ .<sup>9</sup>

Figures 3(a) and 3(b) represent the  $M$ - $H$  curves of  $\text{CeOs}_2\text{Al}_{10}$  and  $\text{CeRu}_2\text{Al}_{10}$  for  $H \parallel a$  at  $T=1.3$  K, respectively. In Fig. 3(a), those at 30 K and 35 K are also shown and in Fig. 3(b), that for  $H \parallel c$  is also shown. While both compounds show the concave  $M$ - $H$  curve for  $H \parallel a$ , a concave  $H$  dependence is much more pronounced in  $\text{CeOs}_2\text{Al}_{10}$  than in  $\text{CeRu}_2\text{Al}_{10}$ . The dashed straight lines highlight the difference of the degree of the concave  $H$  dependence in two compounds. See also caption in Fig. 3. The concave  $H$  dependence is also seen at 30 K and 35 K which is above  $T_0$ , although such an  $H$  dependence is not seen in  $\text{CeRu}_2\text{Al}_{10}$  above  $T_0$ .<sup>9,14</sup> Although the  $M$ - $H$  curve for  $H \parallel c$  is not measured in  $\text{CeOs}_2\text{Al}_{10}$ , it is expected to be similar to that in  $\text{CeRu}_2\text{Al}_{10}$  from the small magnitude of the magnetization, apart from a small anomaly at  $H^*=4$  T and 6 T in  $\text{CeRu}_2\text{Al}_{10}$  and  $\text{CeOs}_2\text{Al}_{10}$ , respectively.<sup>13-15</sup> Also for  $H \parallel b$ , an  $H$ -linear  $M$ - $H$  curve is expected. The concave  $M$ - $H$  curve is the charac-

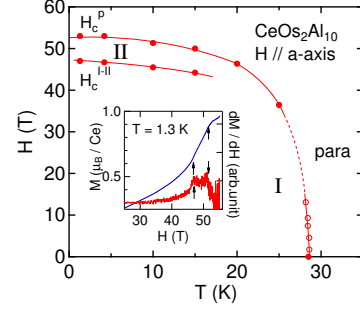


FIG. 2. (Color online) Magnetic phase diagram of  $\text{CeOs}_2\text{Al}_{10}$  for  $H \parallel a$ -axis. The open red circles below 14 T are cited from ref. 13. The inset shows the magnetization curve (blue line) and derivative  $dM/dH$  (red line) at  $T=1.3$  K.

teristic feature for  $H \parallel a$  in these two compounds.

Figure 4 represents the  $T$  dependence of  $\chi$  of  $\text{CeRu}_2\text{Al}_{10}$  and  $\text{CeOs}_2\text{Al}_{10}$  along the  $a$ -,  $b$ - and  $c$ -axes. The results show a large anisotropic behavior,  $\chi_a > \chi_c > \chi_b$  in all the  $T$  region. At high temperatures,  $\chi_c$  and  $\chi_b$  show a similar  $T$  dependence in both compounds. Along the  $a$ -axis, a Curie-Weiss behavior is more pronounced in  $\text{CeRu}_2\text{Al}_{10}$  than in  $\text{CeOs}_2\text{Al}_{10}$ . The magnitude of  $\chi_a$  in  $\text{CeOs}_2\text{Al}_{10}$  at  $\sim T_0$  is much smaller than that in  $\text{CeRu}_2\text{Al}_{10}$ . These indicate that Ce ion in  $\text{CeOs}_2\text{Al}_{10}$  is closer to the valence fluctuation regime than in  $\text{CeRu}_2\text{Al}_{10}$ . A clear broad maximum is seen at  $\sim 40$  K along the  $a$ - and  $c$ -axes in  $\text{CeOs}_2\text{Al}_{10}$ . The  $T$  dependence of  $\chi_a$  at  $\sim T_0$  is very different between two compounds. In  $\text{CeRu}_2\text{Al}_{10}$ , a clear anomaly is seen at  $T_0$  and a rapid decrease below  $T_0$ . On the other hand, in  $\text{CeOs}_2\text{Al}_{10}$ , a continuous decrease is seen down to  $\sim 20$  K without showing an anomaly at  $T_0$ . The dotted lines for  $\chi_a$  are drawn assuming that the paramagnetic state continues to exist down to  $T=0$  K. Their extrapolation to  $T=0$  K is determined from the slope of the dotted straight lines in the  $M$ - $H$  curves in Fig. 3. Namely, the dotted lines in Fig. 3 corresponds to the  $T$  dependence of  $\chi_a$  just above  $H_c^p$ , where the paramagnetic state is realized. We note that the size of the area below the dotted line above the experimental result in Fig. 4 seems to correspond to that in the  $M$ - $H$  curve in Fig. 3 in both compounds.

Now, we discuss the relation between the large spin gap ( $\Delta_{SG}$ ) below  $T_0$  observed in inelastic neutron scattering and the present results of magnetization, because these two are expected to be associated with each other closely. The relation between  $\Delta_{SG}$  and the Kondo temperature,  $T_K = 3T_{\text{max}}$  was discussed in ref. 12. The origin of  $\Delta_{SG}$  is difficult to be ascribed to an anisotropy gap of a magnon branch for the following reasons. The anisotropy of  $\chi$  in  $\text{CeOs}_2\text{Al}_{10}$  is smaller than that in  $\text{CeRu}_2\text{Al}_{10}$  at low temperatures. The magnitude of the magnetic moment at  $H_c^p$  and the ordered moment is smaller in  $\text{CeOs}_2\text{Al}_{10}$  than in  $\text{CeRu}_2\text{Al}_{10}$ .<sup>11,12,16</sup> These suggest that  $\text{CeOs}_2\text{Al}_{10}$  is closer to the valence fluctuation regime than  $\text{CeRu}_2\text{Al}_{10}$ . This is also supported by the pressure effect of the electrical resistivity of  $\text{CeRu}_2\text{Al}_{10}$ .<sup>3</sup> These strongly suggest that the magnetic anisotropy in the ordered state is smaller in

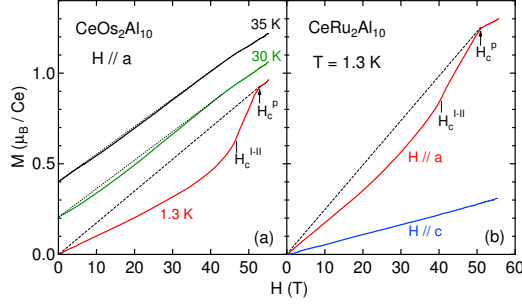


FIG. 3. (Color online) (a) Magnetic field dependence of the magnetization of  $\text{CeOs}_2\text{Al}_{10}$  at  $T = 1.3$  K for  $H \parallel a$ -axis. Those at  $T = 30$  K and  $35$  K are also shown. The dotted lines for the results at  $T = 30$  K and  $35$  K are drawn only to see the concave  $H$  dependence in these results. (b) Magnetization curve of  $\text{CeRu}_2\text{Al}_{10}$  at  $T = 1.3$  K for  $H \parallel a$ -axis (red line) and  $c$ -axis (blue line). The data are cited from refs. 9 and 14. The dashed straight lines in Fig. 3 (a) and (b) are drawn by connecting the origin at  $H = 0$  and  $M$  at  $H_c^p$ .

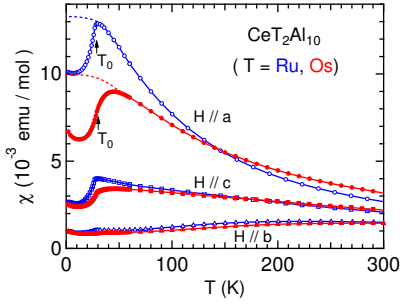


FIG. 4. (Color online) Temperature dependence of the magnetic susceptibility of  $\text{CeRu}_2\text{Al}_{10}$  and  $\text{CeOs}_2\text{Al}_{10}$  along the  $a$ -,  $b$ - and  $c$ -axes measured at 1 T. As for the dotted lines in  $\chi_a$ - $T$ , please see the text in details.

$\text{CeOs}_2\text{Al}_{10}$  than in  $\text{CeRu}_2\text{Al}_{10}$ . This leads to a smaller magnon gap in  $\text{CeOs}_2\text{Al}_{10}$  than in  $\text{CeRu}_2\text{Al}_{10}$ . However, experimentally a larger  $\Delta_{\text{SG}}$  is seen in  $\text{CeOs}_2\text{Al}_{10}$  than in  $\text{CeRu}_2\text{Al}_{10}$ . Considering the fact that  $\text{CeOs}_2\text{Al}_{10}$  is closer to the valence fluctuation regime and  $T_0$  is higher in  $\text{CeOs}_2\text{Al}_{10}$  than in  $\text{CeRu}_2\text{Al}_{10}$ , the hybridization between conduction band and nearly localized  $4f$  shell ( $c$ - $f$  hybridization) is expected to be associated with the origin of the large  $\Delta_{\text{SG}}$ . By applying pressure to  $\text{CeRu}_2\text{Al}_{10}$ ,  $T_0$  increases and the physical properties become closer to those in  $\text{CeOs}_2\text{Al}_{10}$ .<sup>3</sup> This indicates that the Ce-Ce interaction is enhanced by increasing the  $c$ - $f$  hybridization. This is different from many Ce compounds where the transition temperature is suppressed by pressure as a result of the suppression of the RKKY interaction by the Kondo effect.

Based on these considerations, we discuss the magnetization of  $\text{CeT}_2\text{Al}_{10}$ . If the AFM order with  $M_{\text{AF}} \parallel c$  were realized at  $H = 0$ , a spin canting magnetization process would occur for  $H \parallel a$  up to  $H_c^p$ . The  $M$ - $H$  curve of the present compounds show a pronounced concave  $H$  dependence above

$\sim 30$  T and another phase transition at  $H_c^{\text{I-II}}$  appears little below  $H_c^p$ . Such an  $M$ - $H$  curve for  $H \parallel a$  is difficult to explain by a spin canting magnetization process. In order to explain the concave  $M$ - $H$  curve in a spin canting magnetization process, the magnitude of the magnetic moment should increase accompanied with a decrease of a spin canting angle. The  $T$  dependence of  $\chi_a$ , which is expected for  $\chi_{\perp}$ , is not seen in phase I but only seen in phase II. Such a spin canting magnetization process seems unphysical. Then, we expect that the origin of the concave  $M$ - $H$  curve is ascribed to the existence of the large spin gap. First, we discuss the  $T$  dependence of  $\chi$  below and above  $T_0$ .  $\chi_a$  and also  $\chi_c$  show a broad maximum at  $T_{\text{max}} \sim 40$  K. The decrease of  $\chi$  below  $T_{\text{max}}$  indicates that the spin degrees of freedom is suppressed with decreasing temperature even in the paramagnetic region. As its origin, the singlet formation could be considered. Considering that a broad maximum is seen in  $\chi_a$  and  $\chi_c$ , the  $c$ - $f$  hybridization in the  $ac$ -plane may play an important role below  $T_{\text{max}}$ . This is consistent with our previous pointing out that this system is viewed as the  $ac$ -plane two dimensional system stacked along the  $b$ -axis.<sup>8</sup> The decrease of  $\chi_a$  and  $\chi_c$  below  $T_{\text{max}}$  in  $\text{CeOs}_2\text{Al}_{10}$  is expected to be associated with the appearance of a large spin gap in the paramagnetic region. We expect that the spin gap observed in inelastic neutron scattering continues to exist up to  $T_{\text{max}}$ . The ratio of  $T_0 = 27.3$  K in  $\text{CeRu}_2\text{Al}_{10}$  to  $T_{\text{max}} \sim 40$  K in  $\text{CeOs}_2\text{Al}_{10}$  shows a good correspondence to the ratio of  $\Delta_{\text{SG}} = 8$  meV in the former to 11 meV in the latter.<sup>10,12</sup> In ref. 12 on  $\text{CeOs}_2\text{Al}_{10}$ , it is noted the possibility that the inelastic peak exists at  $T_0$ . Thus, we conjecture that in  $\text{CeOs}_2\text{Al}_{10}$ , a spin gap appears below  $T_{\text{max}}$ . This should be examined by the inelastic neutron scattering experiments. The concave  $M$ - $H$  curve for  $H \parallel a$  remains even in the paramagnetic region up to  $T_{\text{max}}$ . This comes from the same origin as a decrease of  $\chi_a$  below  $T_{\text{max}}$ . The  $T$  dependence of  $\chi_a$  of  $\text{CeRu}_2\text{Al}_{10}$  is very different from that of  $\text{CeOs}_2\text{Al}_{10}$ . We measured the pressure effect of  $M$  of  $\text{CeRu}_2\text{Al}_{10}$  for  $H \parallel a$ . When the pressure is applied to  $\text{CeRu}_2\text{Al}_{10}$ , the magnitude of  $M$  is suppressed and becomes to show a broad maximum above  $T_0$ . The magnetic properties of  $\text{CeRu}_2\text{Al}_{10}$  become closer to those of  $\text{CeOs}_2\text{Al}_{10}$  in the same way as in the pressure effect of the electrical resistivity.<sup>3</sup> As the  $c$ - $f$  hybridization is enhanced by applying pressure, the different behavior of  $\chi_a$  around  $T_0$  between  $\text{CeOs}_2\text{Al}_{10}$  and  $\text{CeRu}_2\text{Al}_{10}$  could be understood as a result of a different magnitude of the  $c$ - $f$  hybridization. As the  $c$ - $f$  hybridization should be associated with the singlet formation, the above mentioned singlet is considered to be a Kondo singlet as discussed in ref. 12. Considering that  $\chi_a$  shows a continuous decrease without showing an anomaly at  $T_0$ , the decrease of  $\chi_a$  below  $T_0$  is also dominated by the same mechanism as that above  $T_0$  below  $T_{\text{max}}$ . From these results, we propose that the Kondo singlet accompanied with a spin gap begins to be formed below  $T_{\text{max}}$  and coexists with  $M_{\text{AF}}$  component parallel to the  $c$ -axis in the ordered state. As for  $\chi_c$ , although a broad maximum is seen at  $T_{\text{max}}$ , a rapid decrease is observed below  $T_0$  different from no anomaly in  $\chi_a$ . This rapid decrease of  $\chi_c$  below  $T_0$  may originate from  $M_{\text{AF}} \parallel c$  below  $T_0$ . Now, as it is clear that the origin of the concave  $M$ - $H$  curve for  $H \parallel a$  below  $T_0$  is the same as that of the de-



crease of  $\chi_a$  below  $T_{\max}$ , we could ascribe the former to the existence of a Kondo singlet in the ordered state. Namely, the destruction of a Kondo singlet by the magnetic field induces the concave  $H$  dependence of  $M$ . The degree of the concave  $H$  dependence is much more pronounced in  $\text{CeOs}_2\text{Al}_{10}$  than in  $\text{CeRu}_2\text{Al}_{10}$ . This may indicate that the weight of the singlet component in the ordered state is larger in the former than in the latter.

Next, we discuss the reason why  $M_{\text{AF}} \parallel c$  is realized in the ordered state despite a large anisotropy of  $\chi$ ,  $\chi_a > \chi_c > \chi_b$ , in the paramagnetic region. The fact that  $M_{\text{AF}} \parallel c$  means that the anisotropic exchange interaction should exist and that along the  $c$ -axis,  $J_{\text{ex}}^c$  is largest. However,  $J_{\text{ex}}^c$  is considered to be not strong enough to fix  $M_{\text{AF}}$  to the  $c$ -axis tightly. This comes from the  $\theta$  dependence of  $M$  of  $\text{CeRu}_2\text{Al}_{10}$  in the  $ab$ ,  $bc$  and  $ca$  planes at constant temperatures below and above  $T_0$ . Here,  $\theta$  is the angle between the applied  $H$  direction and the crystal axis in each plane. We observed the smooth  $\theta$  dependence of  $M$  following  $\cos \theta$  in all the planes. The  $\theta$  dependence below  $T_0$  is very similar to that above  $T_0$ . This indicates that the anisotropic exchange interaction which forces  $M_{\text{AF}}$  along the  $c$ -axis in the ordered state is small. Then, we propose the following explanation. In  $\text{CeOs}_2\text{Al}_{10}$ , the magnitude of the reduction of  $\chi$  down to  $T_0$  below  $T_{\max}$  is  $\sim 15\%$  and  $\sim 5\%$  for  $H \parallel a$  and  $H \parallel c$ , respectively. This means that the suppression of the spin degrees of freedom in the paramagnetic region below  $T_{\max}$  is larger along the  $a$ -axis than along the  $c$ -axis. By considering that the suppression of the spin degrees of freedom comes from the  $c$ - $f$  hybridization, the larger hybridization along the  $a$ -axis could make a magnetization easy axis along the  $c$ -axis in place of the  $a$ -axis expected from the largest magnitude of  $\chi_a$  in the paramagnetic region.

Next, we comment the possible origin of the large anisotropic magnetic susceptibility of  $\text{CeT}_2\text{Al}_{10}$  in the paramagnetic region.  $\chi$  of  $\text{CeT}_2\text{Al}_{10}$  with a large anisotropy indicates that the crystalline electric field (CEF) splitting is large. On the other hand, our recent results of the magnetization and thermal expansion of  $\text{NdT}_2\text{Al}_{10}$  ( $T=\text{Ru, Os}$ ) whose  $T_N$  is 2.4 K and 2.2 K in  $\text{NdRu}_2\text{Al}_{10}$  and  $\text{NdOs}_2\text{Al}_{10}$ , respectively indicate that the CEF splitting in  $\text{NdT}_2\text{Al}_{10}$  is small.<sup>17</sup> The Curie-Weiss law with  $\mu_{\text{eff}} \sim 3.65\mu_B/\text{Nd}$  which is close to that of a free Nd ion is observed above  $\sim 100$  K along all the crystal axes in both compounds. The distortion below  $T_N$  is as small as  $10^{-6}$ . These results indicate that the coupling between the lattice and the orbital moment of Nd ion is very small and the

Nd ion behaves as a rather free ion, which may come from the caged structure surrounded by Al and T ions. From these results, the Coulomb interaction as the origin of the CEF splitting is expected to be small also in  $\text{CeT}_2\text{Al}_{10}$ , which contradicts with the large anisotropic magnetic susceptibility. Thus, we expect that in  $\text{CeT}_2\text{Al}_{10}$ , a  $c$ - $f$  hybridization effect is associated with the large CEF splitting. The same  $c$ - $f$  hybridization effect may be also associated with the opening of a spin gap below  $T_{\max}$  and the phase transition at  $T_0$ . Thus, the long range order in  $\text{CeT}_2\text{Al}_{10}$  seems to be dominated by the unusual Ce-Ce interaction.

Finally, we comment the CDW transition proposed by Kimura *et al.* quite recently.<sup>18</sup> Although the optical conductivity clearly shows that the electronic structure along the  $b$ -axis is modulated, the CDW transition along the  $b$ -axis seems difficult from the following results in  $\text{CeRu}_2\text{Al}_{10}$ .<sup>3,8</sup> The electrical resistivity shows a clear enhancement below  $T_0$  along all the crystal axes. The largest enhancement is seen not along the  $b$ -axis but along the  $c$ -axis. The Hall resistivity measured in  $H \parallel a$  where the Hall current is in the  $bc$  plane does not show an anomaly at  $T_0$ .<sup>8</sup> Although these are the results in  $\text{CeRu}_2\text{Al}_{10}$ , considering that the same type of LRO is strongly expected in these two compounds, the above results are difficult to understand by the CDW transition along the  $b$ -axis. The fact that the temperature where a charge gap along the  $b$ -axis begins to open coincides with  $T_{\max}$  of  $\chi_a$  and  $\chi_c$  in the present experiments indicates a close relation between a charge gap and a spin gap in a novel phase transition in this system.

In summary, we have studied the magnetization of  $\text{CeOs}_2\text{Al}_{10}$  up to 55 T for  $H \parallel a$ . The concave  $M$ - $H$  curve is observed not only below  $T_0$  but in a paramagnetic region below  $T_{\max}$  where  $\chi_a$  and  $\chi_c$  exhibit a maximum. We proposed that a Kondo singlet accompanied with a spin gap is formed below  $T_{\max}$  and coexists with the AFM order below  $T_0$ . As the origin of the AFM order with  $M_{\text{AF}} \parallel c$  at  $H=0$ , we propose the larger suppression of the spin degrees of freedom along the  $a$ -axis than along the  $c$ -axis.

From very recent inelastic neutron scattering experiments by P. Deen *et al.*<sup>19</sup>, we note that the spin gap in  $\text{CeOs}_2\text{Al}_{10}$  is clearly open at  $T = 35$  K. This observation rules out a simple magnon gap below  $T_0$  as a possible explanation for the observed spectral response in the inelastic neutron scattering experiments, thus implying that it should result from a spin singlet formation.

\* kondo@issp.u-tokyo.ac.jp

<sup>1</sup> A. M. Strydom, *Physica B* **404**, 2981 (2009).

<sup>2</sup> Y. Muro *et al.* *J. Phys. Soc. Jpn.* **78**, 083707 (2009).

<sup>3</sup> T. Nishioka *et al.* *J. Phys. Soc. Jpn.* **78**, 123705 (2009).

<sup>4</sup> M. Matsumura *et al.* *J. Phys. Soc. Jpn.* **78**, 123713 (2009).

<sup>5</sup> H. Tanida *et al.* *J. Phys. Soc. Jpn.* **79**, 043708 (2010).

<sup>6</sup> K. Hanzawa, *J. Phys. Soc. Jpn.* **79**, 043710 (2010).

<sup>7</sup> S. Kambe *et al.* *J. Phys. Soc. Jpn.* **79**, 053708 (2010).

<sup>8</sup> H. Tanida *et al.* *J. Phys. Soc. Jpn.* **79**, 063709 (2010).

<sup>9</sup> A. Kondo *et al.* *J. Phys. Soc. Jpn.* **79**, 073709 (2010).

<sup>10</sup> J. Robert *et al.* *Phys. Rev. B* **82**, 100404 (2010).

<sup>11</sup> D.D. Khalyavin *et al.* *Phys. Rev. B* **82**, 100405 (2010).

<sup>12</sup> D. T. Adroja *et al.* *Phys. Rev. B* **82**, 104405 (2010).

<sup>13</sup> Y. Muro *et al.* *Phys. Rev. B* **81**, 214401 (2010).

<sup>14</sup> A. Kondo *et al.* *J. Phys. Soc. Jpn.* **80**, 013701 (2011).

<sup>15</sup> H. Tanida *et al.* *J. Phys. Soc. Jpn.* **79**, 083701 (2010).

<sup>16</sup> J-M. Mignot *et al.* *J. Phys. Soc. Jpn.* in press.

<sup>17</sup> T. Nishioka, *et al.* in preparation.

<sup>18</sup> S. Kimura *et al.* *Phys. Rev. Lett* **106**, 056404 (2011).

<sup>19</sup> P. Deen *et al.* (unpublished).